Clim Dyn (2011) 36:1365–1378
DOI 10.1007/s00382-010-0824-0

Statistical downscaling of sea-surface wind over the Peru–Chile upwelling region: diagnosing the impact of climate change from the IPSL-CM4 model

K. Goubanova · V. Echevin · B. Dewitte · F. Codron · K. Takahashi · P. Terray · M. Vrac

Received: 17 August 2009 / Accepted: 10 April 2010 / Published online: 9 May 2010

Abstract The key aspect of the ocean circulation off Peru–Chile is the wind-driven upwelling of deep, cold, nutrient-rich waters that promote a rich marine ecosystem. It has been suggested that global warming may be associated with an intensification of upwelling-favorable winds. However, the lack of high-resolution long-term observations has been a limitation for a quantitative analysis of this process. In this study, we use a statistical downscaling method to assess the regional impact of climate change on the sea-surface wind over the Peru–Chile upwelling region as simulated by the global coupled general circulation model IPSL-CM4. Taking advantage of the high-resolution QuikSCAT wind product and of the NCEP reanalysis data, a statistical model based on multiple linear regressions is built for the daily mean meridional and zonal wind at 10 m for the period 2000–2008. The large-scale 10 m wind components and sea level pressure are used as regional circulation predictors. The skill of the downscaling method is assessed by comparing with the surface wind derived from the ERS satellite measurements, with in situ wind observations collected by ICOADS and through cross-validation. It is then applied to the outputs of the IPSL-CM4 model over stabilized periods of the pre-industrial, $2 \times CO_2$ and $4 \times CO_2$ IPCC climate scenarios. The results indicate that surface along-shore winds off central Chile (off central Peru) experience a significant intensification (weakening) during Austral winter (summer) in warmer climates. This is associated with a general decrease in intra-seasonal variability.

Keywords Statistical downscaling · Coastal wind · Upwelling · Peru · Chile · Climate change

K. Goubanova (✉) · B. Dewitte
Laboratoire d'Etudes en Géophysique et Océanographie Spatiale, CNES/CNRS/IRD/UPS, Toulouse, France
e-mail: katerina.goubanova@legos.obs-mip.fr

V. Echevin · P. Terray
Laboratoire d'Océanographie et de Climatologie: Expérimentation et Approches Numériques, IPSL/UPMC/IRD, Paris, France

K. Goubanova · B. Dewitte
Instituto del Mar del Peru, Callao, Peru

F. Codron
Laboratoire de Météorologie Dynamique, UPMC/CNRS, Paris, France

B. Dewitte · K. Takahashi
Instituto Geofisico del Peru, Lima, Peru

M. Vrac
Laboratoire des Sciences du Climat et de l'Environnement, IPSL/CNRS/CEA/UVSQ, Gif-sur-Yvette, France

1 Introduction

The coastal ocean off Chile and Peru is characterized by the upwelling of cold, nutrient-rich waters, which drives an exceptionally high biological productivity (Carr 2002). This upwelling is induced by the southerly, nearly along-shore flow associated with the trade winds in the tropics and with the eastern flank of the South-East Pacific (SEP) anticyclone in the mid-latitudes. In particular, Renault et al. (2009) demonstrate that off Central Chile ($\sim$30–35°S) during the austral summer, the low-level along-shore winds control, to a large extent, the upwelling variability through Ekman transport (Barber and Smith 1981) and Ekman pumping (Halpern 2002). The upwelling-favorable winds off Chile exhibit particularly strong intra-seasonal variability related to the intermitted formation of a coastal jet

(CJ) (Garreaud and Munoz 2005; Renault et al. 2009). A similar pattern of wind variability is found off central Peru, although with a reduced meridional extension and a weaker magnitude. Recent observations (VOCALS-Rex cruise, October 2008) suggest that the wind intensification near Pisco (13°7′S, 76°12′W) shares many characteristics with the CJ off Central Chile. As an illustration, Fig. 1a shows the climatological sea-surface wind speed and running variance over the Peru–Chile upwelling region. It highlights the regions of Coastal Jet events with local maxima in mean wind and variance near the coast, namely the Pisco region and the Coquimbo (29°57′S, 71°21′W) region. The two regions experience out of phase seasonal cycles (Fig. 1b) with the strongest along-shore winds occurring in October–March (April–September) in the central Chile (Peru) region. These regions are of particular interest with regards to the impact of climate change because they hold important resources which are likely to be sensitive to changes in the synoptic atmospheric circulation.

It has been suggested in a previous study (Bakun 1990) that global warming may be associated with an intensification of coastal upwelling in eastern boundary upwelling systems (EBUS). The proposed theoretical mechanism is that in a warmer climate the land–sea thermal contrast will increase, which will intensify the cross-shore pressure gradient driving the alongshore upwelling-favorable wind. Such local- and regional effects could be amplified or reduced by changes in the large-scale climate processes affecting the Peru–Chile upwelling region. The climate projections of the International Panel for Climate Change (IPCC) Coupled General Circulation Models (GCM) show an increase in surface pressure just to the south of the SEP anticyclone (Garreaud and Falvey 2009). The resulting increase in meridional pressure gradient drives an intensification of the southerly alongshore flow between about 25°S and 40°S. Such changes of the large-scale forcing are likely to impact the regional wind regime and participate in the intensification of the upwelling along the Chilean coast. On the other hand, in the tropics, the IPCC models predict a reduction of the mean Walker (Vecchi and Soden 2007) and Hadley circulations (Held and Soden 2006; Gastineau et al. 2008) in association with a decrease in extreme wind events (Gastineau and Soden 2009). These changes may alter the wind regime off Peru in a way which cannot be inferred in a straightforward manner. Modeling studies in particular suggest that characteristics of the near-shore along-shore winds off Peru may be influenced by the air–sea interaction associated with oceanic meso-scale variability (cf Chelton et al. 2007 for California current system; Seo et al. 2007). Therefore, how the changes in the large-scale conditions due to global warming will impact the along-shore circulation off the western coast of South America is still an issue of debate, with obvious societal implications.

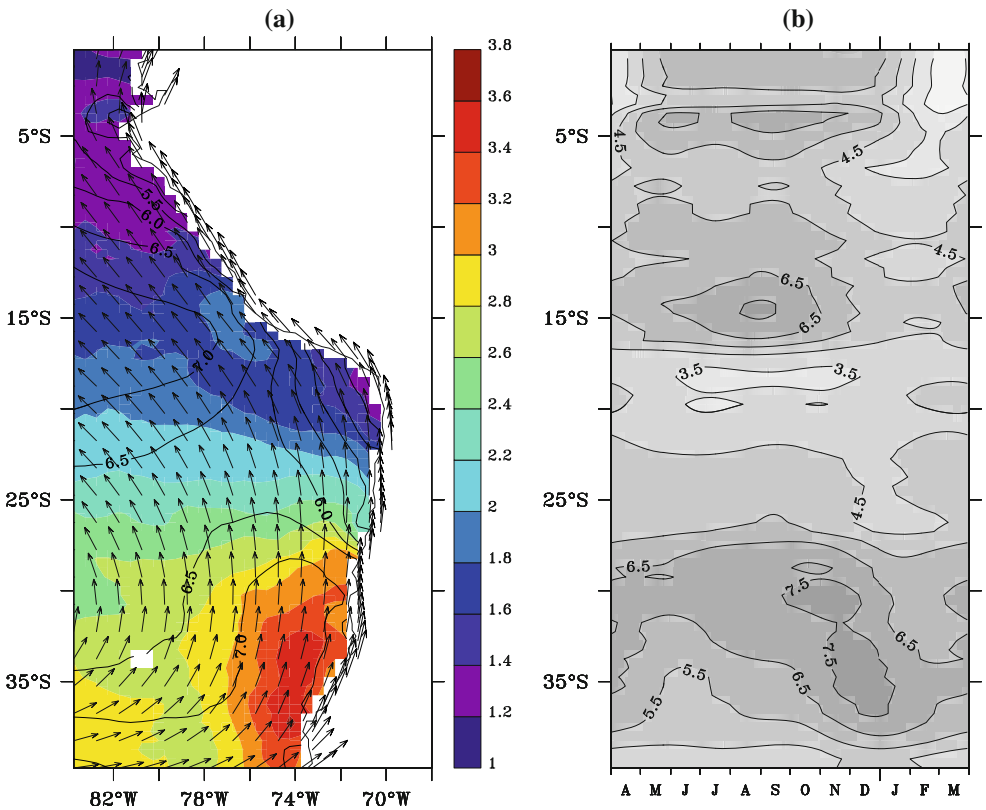

Fig. 1 Surface wind off Chile–Peru coast from QuickSCAT for the period 2000–2008. **a** Mean wind speed (*contours*), wind speed intraseasonal variability (*colors*) and direction of mean wind (*arrows*). Intraseasonal variability is calculated as climatological 15 day running variance of wind speed anomalies. The *thick arrows* on the land indicate the mean wind direction at the first grid point close to shore. Units: m/s. **b** Mean seasonal cycle of the wind speed along the west coast of South America calculated by the projection on the near alongshore direction indicated by *thick arrows* in (**a**). Average of the three grid points close to shore is shown. Units: m/s. The figure indicates two regions of coastal jet events: at ∼15°S and between 30 and 37°S

Although the global coupled models from the IPCC have provided meaningful information on the potential impact of climate change on the large-scale atmospheric circulation, they cannot be used directly to infer impact on the surface wind regime along the coast because of their too coarse resolution. In particular, CJ events, which are characterized by a horizontal scale ($\sim$300 km) (Renault et al. 2009) comparable to the typical size of a GCM grid cell, cannot be resolved properly by coupled models. Downscaling the GCMs projections is thus necessary in order to provide a more quantitative estimate of the regional impact of climate change in the Peru–Chile upwelling region. Whereas dynamical downscaling is, in general, heavy to implement due to the computational costs associated with the use of high-resolution atmospheric models, statistical downscaling offers a cost-effective alternative. Only few recent studies use statistical downscaling techniques to estimate the local change in surface wind associated with global warming (Sailor et al. 2000; Pryor et al. 2005, 2006; Najac et al. 2009; Salameh et al. 2009). These studies are generally focused on land regions and are motivated by the increasing interest to assess impact of climate change on wind power potential. Note also the recent studies by Cassou et al. (2010) and Minvielle et al. (2010) who applied a statistical downscaling method to reconstruct high resolution atmospheric forcing over the Atlantic for the period 1958–2002.

In this paper, we use a statistical downscaling method to assess the impact of climate change on the sea-surface wind over the Peru–Chile upwelling region with a focus on the regions of Coastal Jets, namely Central Peru and Central Chile. The paper is organized in the following way. In the next section, we describe the data used in this study. The description of the downscaling method, which includes the choice of the predictor variables and predictor domains, is presented in Sect. 3. In Sect. 4, the skill of the statistical model to reproduce some aspects of the synoptic surface circulation is assessed. The results of the downscaling experiments for present-day and future conditions are presented in Sect. 5. A discussion followed by concluding remarks are provided in Sect. 6.

2 Data description

2.1 QuickSCAT and ERS winds:

Statistical downscaling methods are based on a statistical relationship between large-scale climate information and regional near-surface variables of interest. The regional surface wind (zonal and meridional components) for the period 2000–2008 is derived from the QuikSCAT satellite products with a 0.5° × 0.5° spatial resolution. These products are obtained by interpolation of the wind field from polar orbit satellite data covering global ocean on a rectangular grid. The 0.5° resolution land mask was computed from the GMT coastline database. There is no data for grid points located within 25 km of the coastline (satellite blind zone). Our region of interest extends from 5°S to 40°S and from 90°W to 68°W. To validate the downscaling method, we used weekly ERS wind with 1.0° × 1.0° resolution over the period 1992–1999. Both datasets were obtained from the CERSAT database (http://www.ifremer.fr/cersat). More details on the datasets are provided in CERSAT (2002a, b).

2.2 ICOADS wind

The observed wind for the period 1960–2006 collected by the International Comprehensive Ocean–Atmosphere Data Set (ICOADS) (Worley et al. 2005) is also used for validation purpose. ICOADS is a gridded monthly dataset of the world's in situ surface marine observations, which sampling varies regionally ranging from zero to several thousand samples per 1° × 1° box per calendar month. The validation is performed over two regions extending about 3 degrees offshore and corresponding to the CJ zones (between 12.5°S and 15.5°S for Peru and between 28.5°S and 36.5°S for Chile). Although ICOADS has limitations due to the sampling effect of the merchant-ship tracks, it is the only reliable wind product that extends back to 1960 and that allows assessing to some extent the realism of the statistical model for sub-seasonal and interannual timescales.

2.3 NCEP/NCAR and ERA40 Reanalysis

The large-scale sea-level pressure (SLP) and wind components at 10 m over the 131°W–63°W, 16°N–52°S region are extracted from NCEP/NCAR reanalysis (Kalnay et al. 1996) with 2.5° × 2.5° resolution. In the next section, we discuss the choice of these predictors and the size of the predictor area. The sensitivity of the statistical downscaling to the predictor products is tested for the 1992–1999 period using the large-scale predictors, SLP and wind components at 10 m, from ERA40 (Uppala et al. 2005) reanalysis with 1.25° × 1.25° spatial resolution.

2.4 IPCC runs

In order to estimate the change of wind conditions related to anthropogenic greenhouse gases increase, we consider the IPCC CO_2 quadrupling (4 × CO_2) scenario relative to the pre-industrial (PI) simulation for the IPSL-

CM4 model (Marti et al. 2010). The $4 \times CO_2$ run is initialized from the PI one. CO_2 is increased at a rate of 1% per year. After reaching four times the PI concentration the CGCM holds CO_2 fixed for an additional 150 year period to examine the long term response of the climate system. In order to verify if the change in wind is linear from PI to $4 \times CO_2$ climates the stabilized CO2 doubling ($2 \times CO_2$) simulation is also analyzed. A 30 year period was arbitrarily chosen for each experiment over the stabilized time window: 1970–1999 for PI, 2050–2079 for the $2 \times CO_2$ and 2120–2149 for the $4 \times CO_2$. The validation of the CGM was performed using the control climate scenario 20C3M (1970–1999). The motivation for choosing the IPSL-CM4 model was twofold: (1) the daily outputs were available over an extended period of time, and for many variables which allowed carrying numerous tests for the predictors choice; (2) this model has been shown to reproduce realistically some aspects of the large scale circulation (cf. Sect. 3), which includes the ENSO variability (Belmadani et al. 2010), and the subtropical anticyclone (Garreaud and Falvey 2009). Moreover, Fig. 2 shows that the spatial patterns of changes from the present-day conditions to a warmer climate in SLP and SST in the IPSL model are similar to those obtained from a multi-model ensemble [compare Fig. 2 with Fig. 7c of Falvey and Garreaud (2009)]: a reduced warming in SST occurs to the west of the Chilean coast (about 0.05°C/decade less than global mean) and the maximum of the change (up to 18 Pa/decade) in subtropical SLP is situated south-west from the mean location of South Pacific anticyclone. The amplitude of the change simulated by the IPSL-CM4 model is slightly weaker than the multi-model ensemble change.

3 Downscaling method

3.1 General strategy

The main idea of statistical downscaling consists in building a statistical relationship between local/regional variables (predictand) and large-scale climate characteristics (predictors) for the present-day climate, and applying this relationship to the large-scale CGCM outputs for a climate scenario of interest. In this study, we build the statistical model for the wind anomalies relative to its seasonal cycle. The model is based on multiple linear regressions (MLR). As predictand, the surface wind from the QuikSCAT satellite is used; this dataset offers the best quality long-term daily time-series for the purpose of this study. The large-scale variables from the GCM present climate simulation (20C3M) cannot be directly used to build the predictor–predictand relationship since the coupled model starts from arbitrary initial conditions and is not sufficiently constrained to simulate fields in "phase" with the real climate. The large-scale predictors covering the QuikSCAT period are therefore obtained from the NCEP reanalysis data. The spatial resolution of the NCEP data is comparable to that of the CGCM used in this study.

Once the MLR relationship between the QuikSCAT regional wind anomalies and appropriate large-scale predictor anomalies from NCEP is established, this relationship is applied to the large-scale predictor variables from the PI and $4 \times CO_2$ IPSL-CM4 simulations. Note that the relationship holds for anomalies relative to the present climate seasonal cycle, therefore PI and $4 \times CO_2$ anomalies are obtained relatively to present climate IPSL-CM4 climatology. The regional PI and $4 \times CO_2$ wind fields derived in such a way thus represent the anomalies of wind

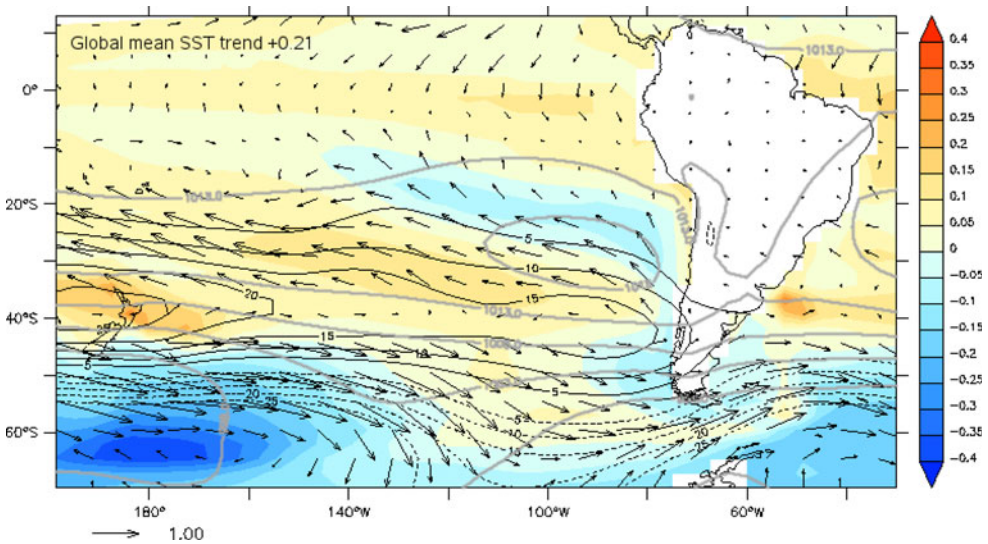

Fig. 2 Differences in anomalous (i.e. global mean substracted) SST (*color*), SLP (*solid/dashed lines*) and 10 m wind (*arrows*) in South-East Pacific between the periods 2070–2099 (A2 scenario) and 1970–1999 (20C3M scenario) simulated by IPSL-CM4 model

relative to the 2000–2008 QuikSCAT seasonal cycle. This procedure assumes that a change in the seasonal cycle can be grasped by the statistical model, namely that changes in the seasonal cycle project onto intra-seasonal and intra- to interannual variability.

3.2 Choice of predictors

An appropriate selection of the predictor variables based on physical consideration is one of the most important steps in the development of a statistical downscaling algorithm. Naturally, predictors for the surface wind have to represent the large scale atmospheric circulation, its main forcing. The relationship between large-scale circulation and regional wind could be more complicated in the coastal zone than offshore, because the orography can modify the surface wind direction and its spatio-temporal characteristics. The regime of along-shore wind over the Peru–Chile region characterized by a relatively simple coastal line exhibits a strong influence of steep and near-shore Andes (Xue et al. 2004) oriented in an approximately north–south direction. Such a boundary does not allow an easterly geostrophic flow to balance the meridional surface pressure gradient associated with the SEP anticyclone. The meridional pressure gradient accelerates instead ageostrophic near surface along-shore coastal jet (Garreaud and Falvey 2009). Note that a strong coupling between surface ocean and surface atmosphere in tropical and coastal region (Small et al. 2008 and references within, Jin et al. 2009) would suggest to include as predictor a high resolution sea surface temperature (SST) to the downscaling scheme. For instance, a statistical relationship between wind stress and SST is proposed in Chelton et al. (2001). However, this could not be done in the present study as the coarse resolution of the CGCMs outputs does not allow representing the nearshore SST meso-scale features which impact the atmospheric boundary layer in the regions of strong coupling.

Hence for our downscaling scheme the large-scale, meridional and zonal wind at 10 m and sea level pressure are chosen a priori as appropriate/reasonable predictors. The winds at 850 and 500 hPa were also tested as potential predictors but this did not improve the results.

To identify the optimal geographic location of the predictor variables, the SLP from NCEP reanalysis are regressed onto the QuikSCAT winds at the two main coastal jet zones (cf. Fig. 1): at 34.25°S 72.25°W and 14.75°S 76.25°W. The results are displayed in Fig. 3. The obtained pattern indicates that the region actively influencing the variability near Pisco corresponds to the mean position of SEP anticyclone, whereas wind over Coquimbo is forced from a region situated southward from the centre of anticyclone, consistently with Renault et al. (2009) (their Fig. 15). Therefore, the downscaling domain for the predictor variables is extended to the south-west (relative to predictand domain) in order to include the zone with the maximum correlation between CJ over Chile and SLP over the SEP and to consider the influence of the South Pacific storms (Fig. 4).

3.3 Statistical model and downscaling procedure

In order to reduce the spatial dimension of the data and to provide spatial homogeneity of downscaling fields, the predictor–predictand relationship is built in the empirical orthogonal functions (EOF) space. The EOFs are computed for the anomalies relative to the mean seasonal cycle for the period 2000–2008. For the predictand, EOFs are obtained based on the covariance matrix containing QuikSCAT zonal and meridional wind anomalies. We retain the first ten EOFs explaining about 75% of total variance (Table 1). The predictor EOF space is represented by the 20 first EOFs (about 70% of total variance) computed from the correlation matrix containing SLP, zonal and meridional wind anomalies from NCEP reanalysis. The NCEP fields were previously interpolated on the IPSL-CM4 grid. The predictor–predictand relationship is built for the principal components corresponding to the retained EOFs and has the form:

$$\mathrm{PCQ}_i = \sum_{j=1}^{20} \alpha_{i,j}\mathrm{PCN}_j + \varepsilon,\ i = 1:10, \qquad (1)$$

where PCQ_i are the ith QuikSCAT PC time series, $\alpha_{i,\,j}$ are the regression coefficients, PCN_j are the PCs of the NCEP time series and ε is the regression error. The Table 1 shows standard errors of the regression[1] Eq. 1 for each of ten QuikSCAT PCs. The first three PCs corresponding to the EOFs that explained together about 55% of total variances are associated with standard error of, respectively, 43.5, 39.6 and 35.4 expressed in PC units. Each of these values corresponds to about 30% of the standard deviation of given predictand PC. Higher PCs which individual impact to total variance is less then 5% are associated with amplitudes of regression error that exceeding 50% of their standard deviation. The regression uncertainties related to regression coefficients estimates were evaluated based on the approximate formula (cf., for instance, Faber (2002)). This source of uncertainties is significantly less important than uncertainties related to the regression errors (not shown).

To downscale the PI and 4 × CO_2 scenarios of the IPSL-CM4 model using this statistical model, we first compute the anomalies of the corresponding IPSL-CM4 predictor

[1] Standard error of regression is defined as the standard deviation of regression error ε.

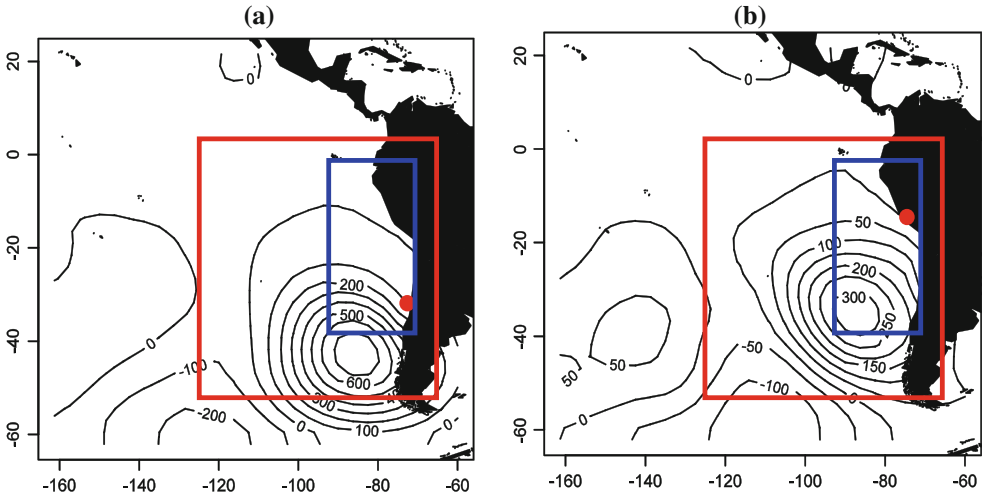

Fig. 3 Regression of sea-level pressure anomalies onto the standardized surface wind anomalies at 34.25°S 72.25°W (**a**) and 14.75°S 76.25°W (**b**) representing, respectively, the Chile and Peru CJ zone. The *blue* and *red rectangles* indicate, respectively, predictand and predictor domains. Units: hPa

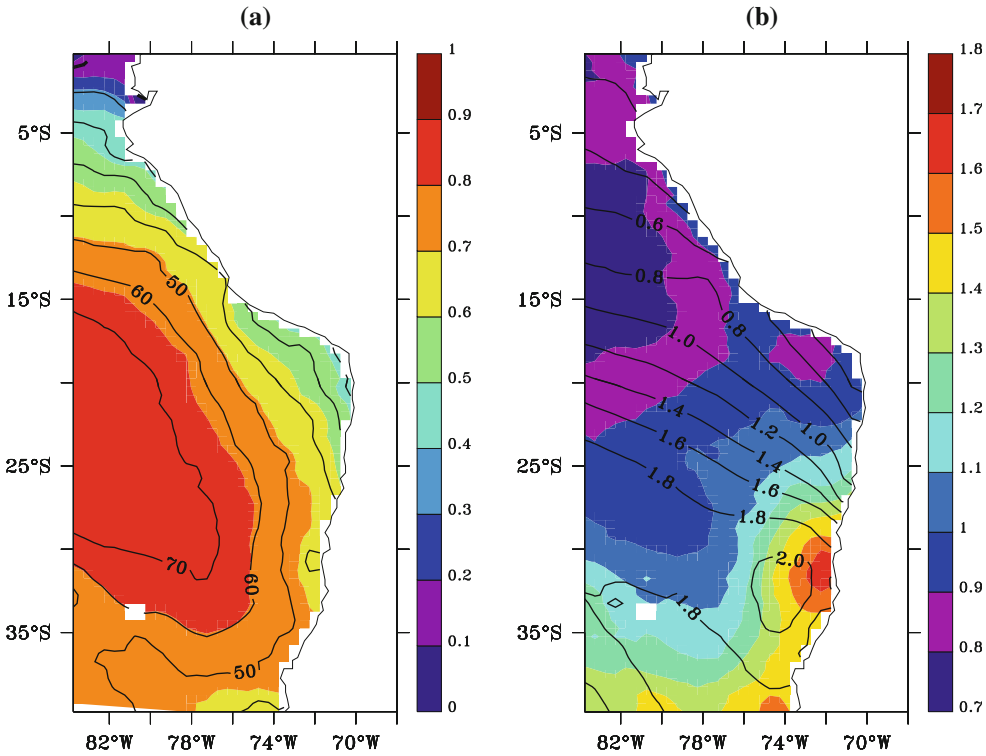

Fig. 4 Maps of correlation (**a** *left panel*) and RMS difference (in m/s, **b** *right panel*, in m/s) between observed by ERS satellite and downscaled wind speed (1992–1999). *Contours* on the *left panel* indicate the percentage of observed variance explained by the downscaled wind. *Contours* on the *right panel* indicate the RMS (in m/s) of the observed wind

variables relative to the seasonal cycle of the present-day climate. The seasonal cycle is derived from the IPSL-CM4 control climate simulation (20C3M run) for the period 1970–1999. The anomalies are then projected onto the predictors EOF space. Applying the regression coefficients to these projections, the time series associated to a given climate scenario can be obtained over the high-resolution domain:

$$\mathrm{PCX}_i = \sum_{j=1}^{20} \alpha_{ij}(X \cdot \mathrm{EOFN}_j),\ i = 1:10, \qquad (2)$$

where X is the anomalies of the IPSL-CM4 predictors for the given climate scenario, EOFN_j is the jth NCEP

Table 1 Statistics of the ten predictand PCs used in the downscaling method

	PC1	PC2	PC3	PC4	PC5	PC6	PC7	PC8	PC9	PC10
EV	25.7	17.7	11.6	4.6	4.2	3.6	2.4	1.8	1.5	1.2
SD	162.3	134.6	108.4	66.0	62.3	59.9	49.2	43.8	39.0	35.2
SE	43.5	39.6	35.4	34.9	39.8	38.9	36.6	35.9	35.2	29.7
SE/SD	27	29	33	53	62	65	74	82	90	84

Percentage of total variance (*EV*) explained by PC, standard deviation (*SD*) (in PC units), standard error (*SE*) (in PC untis) of the regression Eq. 1. The ratio between standard error of the regression and standard deviation of PC (*SE*/*SD*) is also shown (in percents)

eigenfunction. The downscaled fields are finally reconstructed following:

$$Y_{\mathrm{DS}} = \mathrm{PCX} \cdot \mathrm{EOFQ}, \quad (3)$$

where PCX are the time series obtained in Eq. 2, EOFQ are the QuikSCAT eigenfunctions and Y_{DS} are the downscaled anomalies of meridional and zonal wind relative to the present climate seasonal cycle for the given IPSL-CM4 scenario.

The total wind field can be obtained by adding the present-day seasonal cycle as derived from QuikSCAT to the downscaled anomalies.

4 Validation of the statistical model

This section is devoted to the validation of some aspects of the statistical model variability, bearing in mind that observations over this region of the world are either sparse in time and space or do not have the appropriate resolution.

In order to validate the predictor–predictand relationship in Eq. 1 obtained for the 2000–2008 over an independent period, we use the surface wind product from the ERS satellite available from 1992 to 1999. The relationship in Eq. 1 is applied to the NCEP large-scale variables for the period 1992–1999 as described in the previous section for the IPSL-CM4 predictors. The NCEP anomalies for 1992–1999 are computed relative to the 2000–2008 seasonal cycle. Daily downscaled wind is reconstructed on the $0.5° \times 0.5°$ QuikSCAT product grid. To validate the results against weekly ERS data with the $1° \times 1°$ spatial resolution, the weekly averaged surface winds from ERS are bilinearly interpolated on the QuikSCAT grid. Weekly averages of the downscaled product are estimated to compare to the ERS data.

Figure 4a shows the maps of correlation (color) between the downscaled and observed wind speed anomalies and the percentage of wind speed variance explained by the downscaling product (contour). The proportion of explained variance is defined following von Storch and Zwiers (2004):

$$R^2_{\mathrm{FP}} = 1 - \mathrm{var}(F - P)/\mathrm{var}(P),$$

where F is the downscaled field and P the verifying observations. So R is the percentage of observed variance explained by the statistical model.

The correlation between the observations and the downscaled product is greater than 0.6 over most of the region, which indicates that the statistical model exhibits significant skill in reproducing the surface circulation over the 1992–1999 period. The skill is reduced in the coastal region off Northern Chile and off the North and South of Peru where the variability is weaker. An underestimated explained variance indicates a loss of variance in the downscaled product which is inevitable when using linear regression model. Note that this shortcoming could be overcome by adding noise to the model (von Storch 1999) or by using a conditional resampling technique (Minvielle et al. 2009). Figure 4b indicates that the root mean squared error (RMSE) of the downscaled wind (color) does not exceed its RMS (contour) all over the region. Note also that the model biases may originate from biases of the NCEP outputs themselves in this region that the statistical approach cannot fully correct.

Although this study is not focused on the equatorial zone, it is worth noting a weak correlation in the northern part of the studied region. It should be related to the different nature of the atmospheric dynamics in this zone related in particular to the strong coupling between the surface atmosphere and ocean. Based on modes of maximum variability of atmospheric circulation over the Peru–Chile region the model accounts mainly for the signal associated with SEP anticyclone variability and related migratory atmospheric disturbances. In order to represent realistically the equatorial band one should consider separately the tropical and extratropical dynamics (cf. for instance Minvielle et al. (2009)).

As a consistency check of the validation of the daily downscaled wind, a cross-validation over the period 2000–2008 is performed in the following way. One year is skipped from the data (NCEP predictor and QuikSCAT predictand). The relationship in Eq. 1 is fitted to the retained data, and used to downscale the skipped year. This procedure is then repeated for each of the nine years from 2000–2008. The reconstructed 9 year period is then compared with the original QuikSCAT data. The results are very similar to those of the validation against the weekly ERS winds (not shown).

Since the statistical model is constructed using a relatively short time-period (2000–2008), it is important to check its ability to reproduce the inter-annual variability of the wind, which may be a better test than the high-frequency variability for giving confidence in predictions of climate change. In the short record of the ERS data, only a case study for the 1997/1998 El Niño-La Niña is addressed. As an illustration on how the statistical model can grasp some aspects of the surface wind interannual variability, we present the Fig. 5 which shows the difference in wind speed between the warm and cold phases of the 1997/1998 El Niño-La Niña for the observations, the downscaled product and the original NCEP outputs. The downscaled winds keep some of the biases of the raw NCEP product: the intensification of the winds is too weak in the northern part of the domain, and the decrease in speed in the South is too strong. They, however, also show some clear improvements, especially near the coast. The statistical model allows for a reduction of the northerlies off central Chile compared to the NCEP outputs during the 1998/99

La Niña, which is in better agreement with the observations. The most striking improvement brought by the statistical model is the correct positioning of the Central Chile wind core near the coast compared to the NCEP outputs that simulate the wind anomalies too far off-shore. The anomaly pattern is also in overall better agreement with the observations in the downscaled product than in the NCEP outputs, with in particular a more realistic location of the transition zone (zero contour) between positive and negative anomalies. The spatial correlation between the observations and the downscaled product reaches 0.65 whereas it is 0.42 between the observations and the original NCEP outputs interpolated on the $0.5° \times 0.5°$ grid. For the northern part of the domain (Peru region), the positive amplitude of the asymmetry pattern is weaker for the downscaled product than for the observations. This indicates that the method cannot correct for the lack of variability in wind off Peru during the 1997/98 El Niño-La Niña. Note, however, that along the coast, the method gives a better representation of the off-shore gradient in the winds. The Fig. 6(a–c) is similar to Fig. 5 but for a zoom over the Central Peru region. It illustrates the improvement brought by the method which yields a more realistic pattern of coastal wind anomalies.

To test the sensitivity of the statistical relationship Eq. 1 to the predictor products we use the ERA40 reanalysis. ERA40 outputs have a spatial resolution twice higher than the NCEP outputs. Moreover, along the west coast of South America, the large-scale winds in ERA40 are characterized by different spatial patterns than in the NCEP reanalysis and are more realistic during the ERS period. In particular, both zones of coastal jet are better represented by ERA40 (Table 2). To verify if the regional differences of the large-scale predictors would impact the downscaled wind patterns, the relationship Eq. 1 is applied to the large-scale predictors from the ERA40 reanalysis for the period 1992–1999. The ERA40 data were first interpolated on the NCEP grid. The results show a weak sensitivity of the statistical model to the predictor products. As an illustration, the Fig. 6 shows the difference in wind amplitude between the warm and cold phases of the 1997/1998 El Niño-La Niña over the Peruvian coastal jet zone for the NCEP and ERA40 outputs and for the corresponding downscaled fields. Although the NCEP and ERA40 winds have a very different spatial pattern near the coast, the downscaled products lead to comparable anomaly patterns during the 1997/98 El Niño-La Niña, indicating that the statistical model is mostly sensitive to the predictor variables at the synoptic scale.

In order to provide a more quantitative estimate of the model skill for interannual timescales, the NCEP reanalysis is then downscaled on the period 1960–1999 and the results are compared to the ICOADS wind data. Monthly anomalies of meridional wind are compared for two regions centered in the CJ zones (from 12.5°S to 15.5°S and from 30°S to 35°S) and extending for about 3 degrees of longitude offshore. The results are reported in Table 2 for different time periods. The correlation between ICOADS and other data sets over their overlapping periods is also provided in order to highlight the limitation of the ICOADS data set for validation purpose. In particular, over the QuickSCAT period, the correlation between ICOADS and QuickSCAT is as low as 0.40 (0.29) for the Peru (Chile) region with large values of RMSE. The correlation with ERS data is 0.33 and 0.46 for, respectively, Peru and Chile. The comparison for the downscaled products leads to

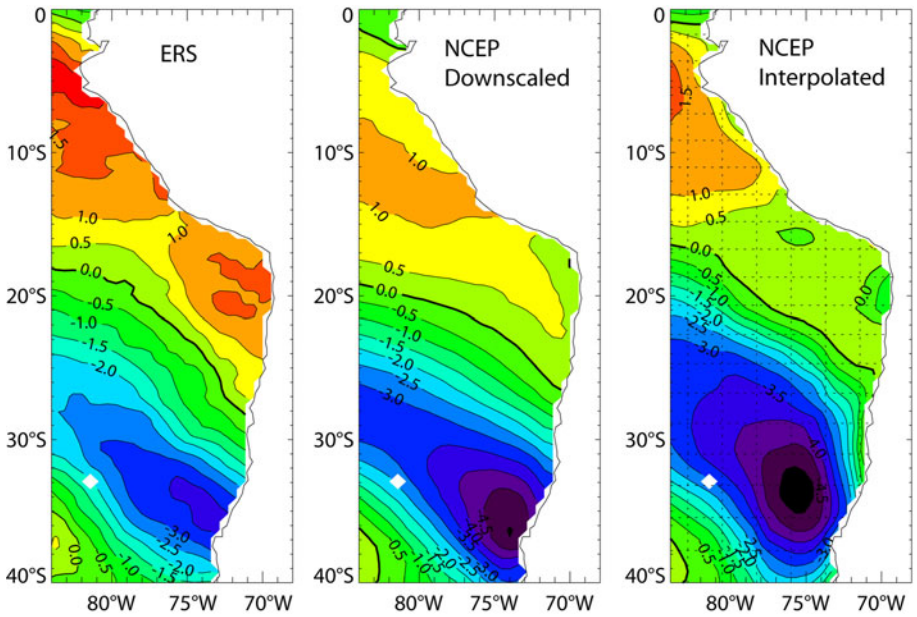

Fig. 5 Maps of the difference in wind amplitude between the warm phase and the cold phase of the 1997/1998 El Niño-La Niña for (from *left* to *right*) the ERS satellite data, the downscaled products and NCEP outputs. Data were 6 month low-pass filtered and the warm (cold) phase corresponds to September 1997 (December 1998). The NCEP outputs were bi-linearly interpolated on the QuickSCAT grid. The graticules of parallels and meridians are drawn on the NCEP map every 2° in order to recall the resolution of the NCEP outputs. Units: m/s

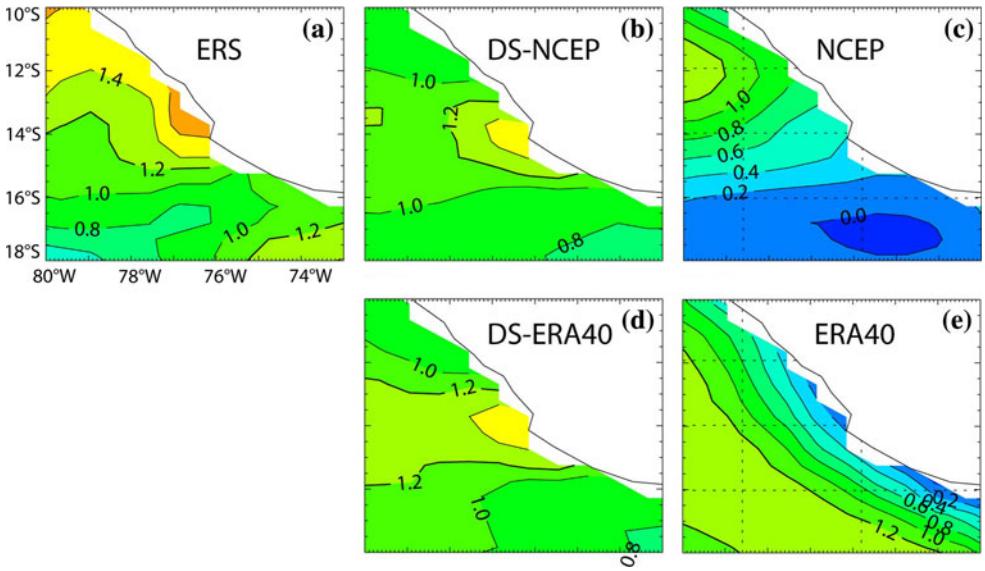

Fig. 6 As in Fig. 5 but zoomed over Central Peru (**a**–**c**). The downscaled products based on the large-scale predictor from ERA40 (**d**) and ERA40 outputs bi-linearly interpolated on the QuikSCAT grid (**e**) are also shown. Units: m/s

Table 2 Comparison of the monthly surface meridional wind between different datasets for the coastal area extending for about 3 degrees of longitude off shore over Central Peru (from 12.5°S to 15.5°S)/Central Chile (from 30°S to 35°S): correlation, RMS for each dataset and RMS difference

Dataset I	Dataset II	Period	Correlation	RMS I (m/s)	RMS II (m/s)	RMS_diff (m/s)
DS_ncep	ICOADS	1960–1999	0.27/0.36	0.37/1.2	0.89/2.14	0.87/2.05
DS_ncep	ICOADS	1992–1999	0.41/0.45	0.31/1.09	1.04/2.34	0.85/1.96
DS_era	ICOADS	1992–1999	0.44/0.49	0.39/1.12	1.04/2.34	0.94/2.04
ICOADS	ERS	1992–1999	0.33/0.46	1.04/2.34	0.51/1.15	0.99/2.08
ICOADS	QuikSCAT	2000–2006	0.40/0.29	1.07/2.28	0.43/1.19	0.98/2.25
NCEP	ERS	1992–1999	0.24/0.77	0.56/1.04	0.51/1.15	0.66/0.76
DS_ncep	ERS	1992–1999	0.59/0.84	0.33/1.09	0.51/1.15	0.42/0.65
ERA	ERS	1992–1999	0.75/0.88	0.42/1.07	0.51/1.15	0.34/0.54
DS_era	ERS	1992–1999	0.70/0.83	0.39/1.12	0.51/1.15	0.37/0.67
NCEP	QuikSCAT	2000–2006	0.17/0.28	0.58/1.04	0.43/1.19	1.13/2.20

DS_ncep (DS_era) indicates wind downscaled based on the large-scale predictor from NCEP (ERA40) reanalysis. All dataset are linearly interpolated on the 1° × 1° ERS grid

comparable values of correlation with ICOADS data, whereas the correlation values are much higher when using the ERS data. These discrepancies are believed to be due to sampling and measurement deficiencies of the ICOADS winds over Peru–Chile ocean region where density of ship-track is rather poor relative to other coastal regions of the global oceans. Despite this, the results of Table 2 reveal that over the 1960–1999 periods, the downscaled product is not in good agreement with ICOADS. Since ICOADS does not either compare well with ERS data and QuickSCAT data, data quality issues could partly explain this low correlation. However, errors can also originate from the NCEP data, therefore it is not possible to draw further conclusions on the realism of the statistical model for the period extended back to 1960.

To summarize, although the statistical model is built from the relative short record of the QuickSCAT data set, it allows simulating some aspects of the intra-seasonal to interannual variability. The model accounts for the large-scale properties of the predictor variables and is weakly sensitive to their regional behavior. It is an important aspect when applying the predictor–predictand relationship to CGCMs having a different spatial resolution. The limitations of the statistical model will be further discussed in the discussion section in the lights of the results of the downscaling experiments of the IPSL-CM4 model.

5 Projection of climate change

In this section, the statistical model is used to assess the impact of anthropogenic greenhouse gases increase on the regional surface winds. The downscaled wind for the

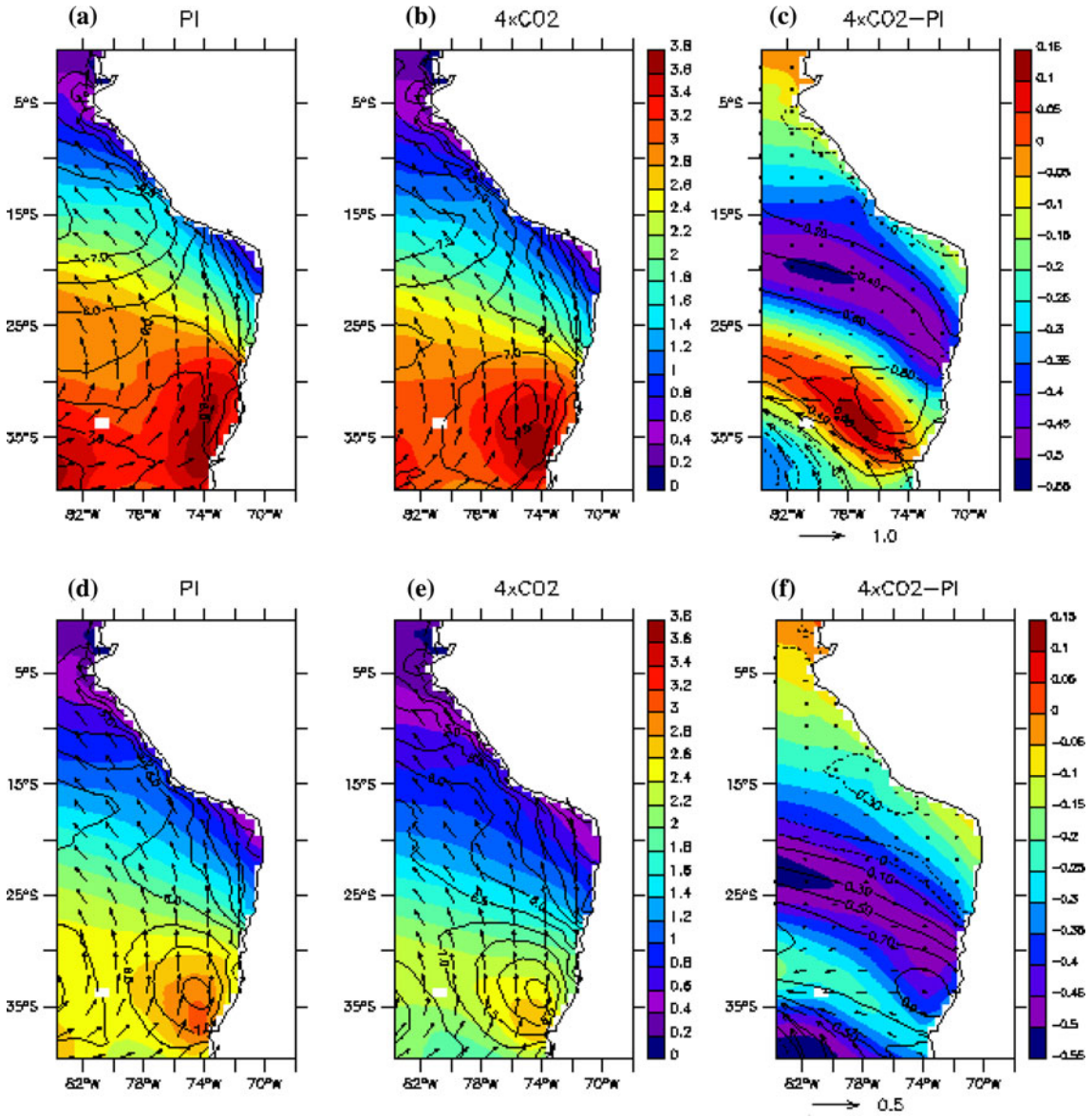

Fig. 7 Surface wind off the Chile–Peru coast for the PI (*left panel*) and 4 × CO_2 (*middle panel*) climate and corresponding differences (*right*): mean wind speed (*contour*), wind speed intra-seasonal variability (*colours*) and direction of mean wind (*arrows*) for winter (*top*) and summer (*bottom*). Units: m/s

4 × CO_2 and PI experiments of the IPSL-CM4 model are estimated and compared. Given that the Peru and Chile CJ seasonal activities are shifted in time (Fig. 1b), the results are first presented for the two contrasted seasons: winter (from April to September) and summer (from October to March) (Fig. 7).

The top panel of Fig. 7 indicates a strong increase of the winter mean wind speed over most of the region with the greatest amplitude off the Central Chile coast. The changes in the wind direction in the southern part of the region correspond to a southward shift of the SEP anticyclone. In summer (Fig. 7, bottom panel) there is also a strong reinforcement of the core of the Chile CJ (up to 1 m/s of wind speed increase), whereas north of about 20°S the wind speed decreases, particularly near the Central Peru Coast. The intra-seasonal variability (indicated by colors in Fig. 7) decreases during both seasons all over the region, except a thin band of weak increasing variance off-shore of Central Chile in winter. It is interesting to note that the change for the 2 × CO_2 climate is characterized by similar spatial patterns with about two times smaller amplitudes (not shown). It implies that the regional surface wind response to global warming is rather linear from the PI to 4 × CO_2 climate.

Changes of the alongshore winds are presented in Fig. 8. The alongshore winds were calculated based on the

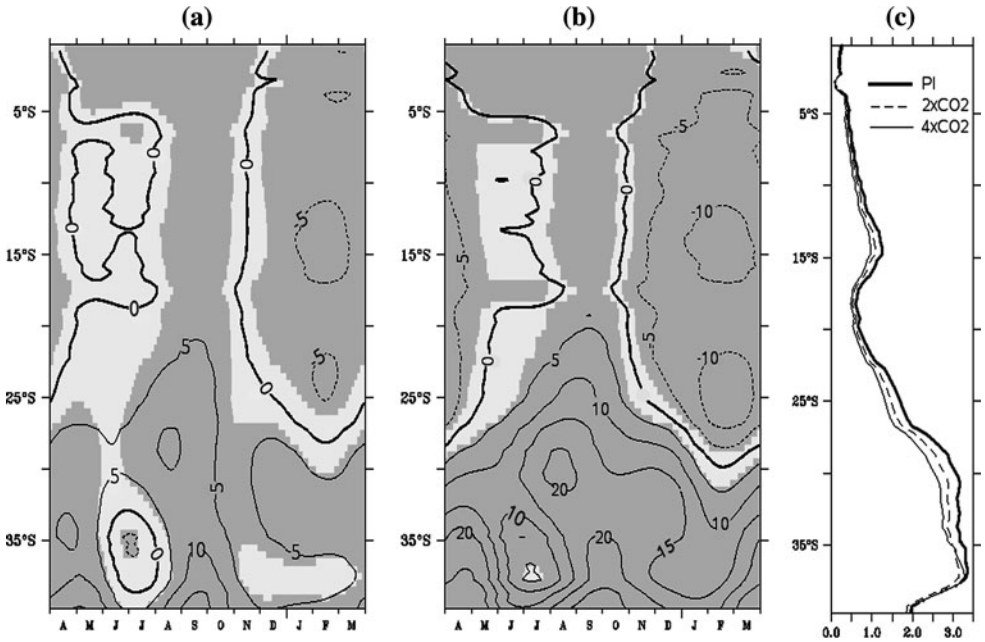

Fig. 8 Change in the along-shore wind speed over the west coast of South America: relative change in mean seasonal cycle (percent) for **a** 2 × CO_2 and **b** 4 × CO_2 relative to PI climate and **c** mean intra-seasonal variability (m/s) for the PI, 2 × CO_2 and 4 × CO_2 climates. The *grey colour* in *panel* **a** and **b** indicates the changes significant at the 0.05 significance level estimated using a bootstrap method (see text). The alongshore wind component is calculated as in Fig. 1b

direction of the mean alongshore winds inferred from the QuikSCAT data (thick arrows on Fig. 1a). Figure 8a, b represent the change in seasonal cycle for 2 × CO_2 and 4 × CO_2 scenarios, respectively. The comparison of these figures suggests the linearity of the response of the along-shore wind to global warming. The changes significant at the 95% level are indicated in shading. Significance level was estimated using a bootstrap method[2] (Efron and Tibshirani 1994). Consistently with recent results obtained from a dynamical downscaling experiment (Garreaud and Falvey 2009), the winds off Central Chile experience a general increase in amplitude with the maximum of change during August–September–October (about 10–20% in the 4 × CO_2 climate). Off Central Peru, the mean wind intensification during austral winter is hardly detectable whereas in austral summer the along-shore winds near Pisco (14°S) experience a decrease in amplitude (up to 12% for the 4 × CO_2 climate). The changes in mean wind amplitude are associated with changes in the intra-seasonal variability (namely CJ activity). Figure 8c shows a decrease of intra-seasonal variability of wind in warmer climates all along the coast with higher magnitudes of change in the 4 × CO_2 than in 2 × CO_2 climate, except the region south of 36°S where the changes in 4 × CO_2 are weak. Interestingly, over Central Chile, these changes can be also evidenced in the distribution of along-shore wind (not shown). For instance, in winter, the skewness of along-shore winds at 35°S changes from positive in the PI climate to negative in the 4 × CO_2 climate. The changes in distribution for both seasons are mainly associated with a decreased frequency of the low (from 0 to 5 m/s) along-shore wind events and an increased frequency of moderate (from 5 to 10 m/s) along-shore wind events (and not for an increase in extreme events). This could be explained by the change in regional circulation due to the southward shift of SEP anticyclone. Indeed, in the PI climate Central Chile is influenced by wind with prevailing zonal component (Fig. 7a) whereas in the 4 × CO_2 climate the wind has mostly a meridional direction parallel to the coast (Fig. 7b). Consequently, when projecting on the along-shore direction, there are less weak wind events in the warmer climate than in the PI one. Over Central Peru the change in along-shore wind distribution consists in a simple shift toward lower values (in summer) and in a decreased width (in winter), without important change of the form.

6 Discussion and conclusions

In this paper, a statistical downscaling method is proposed to assess the impact of climate change on the regional atmospheric circulation of Peru and Chile, taking advantage of the QuickSCAT satellite winds over 2000–2008. The downscaling allows refining the representation of the daily coastal winds for two contrasted scenarios of the

[2] The method consists in creating a surrogate data, namely a randomized data set of along-shore winds by scrambling the original data in the time domain. In the PI run, for the scrambled data set, we select 15 years over the 30-yr record. The seasonal cycle of the along-shore winds is then estimated. The same procedure of scrambling the data set and performing the analysis is repeated 1000 times, which allows deriving the PDF for each calendar month. The distribution is then used to assess the significance level for the change in along-shore winds for each calendar month. .

IPSL-CM4 model, the Pre-Industrial Run and the 4 × CO_2 run. The downscaling method, based on MLR, is applied to anomalies from the present-day climate seasonal cycle. The MLR model's skill is evaluated over the independent ERS period (1992–1999) and over the QuickSCAT period (2000–2008) for which cross-validation is applied. The obtained results are interpreted in the light of the few observational and modeling works available for this region.

It is found that, off Chile, the mean surface winds increase from the PI to the 4 × CO_2 climate. This is consistent with the large-scale conditions that exhibit a strengthening of the meridional pressure gradient over the subtropical Pacific. In a recent study based on dynamical downscaling of the HadCM3 coupled model, Garreaud and Falvey (2009) found a similar tendency, i.e. an increase of the along-shore winds off Chile in a warmer climate. A decrease of the intra-seasonal variability of the coastal jet off Chile is also projected and associated with decreasing (increasing) frequency of occurrence of low (moderate) wind events. These changes could be explained by a general southward displacement of the main climatological structures in the Southern Hemisphere: extension of the Hadley cell (Vecchi and Soden 2007), and poleward shift of the westerly jet and storm tracks (Bengtsson et al. 2006). The CJ region of Central Chile, close to the transition zone between the tropics and the mid-latitudes in the present climate, is subject to a more tropical influence in a warmer climate, and becomes associated to a regime of strong and steady trade winds.

Off Peru, to the authors' knowledge, no comparable downscaling experiment has been documented in the literature, which limits to some extent the interpretation of the obtained results. In the light of our results, a slight decrease in coastal winds is projected to occur off Peru in a warmer climate. This result suggests that in term of impact on the regional along-shore wind off the Peruvian coast, the relaxation of the large-scale tropical circulation predicted for a warmer climate (Vecchi and Soden 2007) prevail over the reinforcement of the SEP anticyclone. It is, however, worth noting that the intuitively expected positive correlation between the equatorial trade winds and the coastal winds off Peru is altered on the ENSO time scale (Bakun and Weeks 2008). It has been shown that the wind stress off Peru increases during El Niño events despite a decrease in the equatorial trade winds (Wyrtki 1975; Bakun and Weeks 2008; see also Fig. 5). Although the dynamical processes driving this response remain unclear, there is the possibility that future change in ENSO characteristics (Yeh et al. 2009) could have a rectified effect on regional mean wind off Peru. Dynamical downscaling for the 20th century is needed in order to better understand the relationship between large-scale circulation and regional wind off Peru on ENSO time scales.

The other main result of this study is a decrease of the intra-seasonal variability of the coastal winds off Peru associated with decreasing mean wind, which could induce a decrease in coastal upwelling. Off Chile, the situation is more complex, the seasonal wind increases whereas the CJ activity decreases. Clearly, experiments using an ocean model are needed to further investigate the impact on coastal upwelling.

One of the main limitations of statistical downscaling is related to the fact that it is based on large-scale information and potential changes in fine-scale processes impacting the along-shore wind are not taken into account. Thus, mesoscale coupling between SST and low level wind (Chelton et al. 2001, 2007) could not be included into the statistical downscaling scheme because of the low resolution of CGCMs predictors. For instance, Seo et al. (2007) shows that in a high-resolution ocean–atmosphere coupled models, SST fronts drive an unambiguous response of the atmospheric boundary layer leading to more realistic surface atmospheric forcings. Since the Peru–Chile region is the siege of an intense mesoscale activity (Chaigneau et al. 2009), such process will need to be taken into account in the future for addressing the issue of the impact of climate change at the regional scale. As a first step towards the development of such dynamical models, SST as simulated by high-resolution oceanic models forced with the wind product presented in this study could be used to improve the statistical approach. This is plan for future work. Note also that besides mesoscale activity, the Peru–Chile coast also experience drastic SST changes associated to equatorial oceanic Kelvin waves. The resulting SST anomalies have also the ability to impact the regional atmospheric circulation. Such process could also be taken into account in the statistical approach.

Another limitation of our approach is related to the treatment of the continent. As a matter of fact, land-sea contrast is assumed to increase under global warming, as enhanced warming may take place over land (Bakun and Weeks 2008). This may drive a cross-shore temperature gradient which reinforces the geostrophic alongshore wind. This potential feedback is not taken into account in our methodology as it would require the use of an atmospheric model that includes a vegetation component. Note that an appropriate dynamical downscaling experiment would allow quantifying the relative impact of land–sea contrast change in increasing trend in wind stress off Peru estimated from in situ data over the 1953–1986 period (Bakun 1990). Indeed, one may argue that this trend could result from the natural variability of the atmospheric circulation in this region, rather than from the impact of climate warming. In particular, a shift in the wind stress time series is clearly visible in the middle of the period (see Fig. 2e–d in Bakun (1990)) and lower trends could be obtained if computed over the two subsequent periods 1953–1971 and 1972–1986. Furthermore, wind stress time series off Peru for the

1949–1972 period, which were calculated by Wyrtki (1975) in an area located slightly further north along the Peruvian coast than the one used by Bakun (1990), do not show any visible trend [see Fig. 3 in Wyrtki (1975)]. Further work based on high-resolution dynamical modeling is clearly required in order to gain confidence in the interpretation of observed trends.

The method is also constrained by the absence of the data in the QuikSCAT product within 25 km from the coastline (satellite blind zone). High-resolution dynamical atmospheric downscaling suggests indeed that within the narrow fringe near the coast, the cross-shore along-shore wind profile can experience drastic changes, leading to wind amplitude significantly lower than the winds at 25 km from the coast (cf. Capet et al. (2004) for the South California coast and Renault (2008) for the Central Chile coast).

Despite the limitations associated to the statistical approach and to the biases of the current generation CGCMs, the proposed downscaling method provides a first approximation of change in regional upwelling favorable wind. The structural significance of the obtained results should be evaluated based on the downscaling of other IPCC models in a future study. Indeed, due to the important range of the climate sensitivity of the CGCMs (Solomon et al. 2007) the deviations among them can be quite relevant.

The proposed method can be easily adapted for other oceanic regions of the world, in particular for the other EBUS, in order to diagnose the impact of climate change on the along-shore winds. It could be interesting to check if similar tendencies are obtained. Due to the cost effectiveness of the method, the ensemble approach is permitted which would allow gaining confidence in the results. Another motivation for this work is the possibility to produce wind products appropriate for the forcing of regional high-resolution ocean models. This would allow a quantitative estimation of the response of the upwelling and regional circulation off Peru and Chile to change in the atmospheric circulation in the context of global warming. This is the topic of on-going research.

Acknowledgments This study was supported by the PCCC (Peru–Chile Climate Change) project funded by the ANR (Agence Nationale de la Recherche) and by the AXA research fund. We would like to thank Sébastien Denvil for providing the IPSL-CM4 data. Stimulating discussions with Sabrina Speich at the early stage of this project and with René Garreaud are also acknowledged. We are also grateful to Ali Belmadani for fruitful discussions.

References

Bakun A (1990) Global climate change and intensification of coastal ocean upwelling. Science 247:198–201

Bakun A, Weeks (2008) The marine ecosystem off Peru: what are the secrets of its fishery productivity and what might its future hold? Prog Oceanogr 79:290–299

Barber RT, Smith RL (1981) Coastal upwelling systems. In: Longhurst AR (ed) Analysis of marine ecosystems. Academic, San Diego, pp 31–68

Belmadani A, Dewitte B, Soon-I An (2010) ENSO feedbacks and associated time scales of variability in a multi-model ensemble. J Clim, (in press)

Bengtsson L, Hodges KI, Roeckner E (2006) Storm tracks and climate change. J Clim 19:3518–3543

Capet X, Marchesiello P, McWilliams J (2004) Upwelling response to coastal wind profiles. Geophys Res Lett, 31, 13 L13309. doi:10.1029/2004GL020303

Carr ME (2002) Estimation of potential productivity in eastern boundary currents using remote sensing. Deep Sea Res II 49:59–80

Cassou C, Minvielle M, Terray L, Perigaud C (2010) A statistical-dynamical scheme for ocean downscaling in the Atlantic. Part I: weather regimes as predictors for surface ocean variables. Clim Dyn. doi:10.1007/s00382-010-781-7

CERSAT (2002a) Mean wind fields (MWF product) user manual volume 1: ERS-1, ERS-2 & NSCAT. Rep C2-MUT-W-05-IF. CERSAT-IFREMER, Brest

CERSAT (2002b) Mean wind fields (MWF product) user manual volume 1: QuikSCAT. Rep C2-MUT-W-04-IF. CERSAT-IFREMER, Brest

Chaigneau A, Eldin G, Dewitte B (2009) Eddy activity in the four major upwelling systems from altimetry (1992–2007). Prog Oceanogr 83:117–123

Chelton DB, Esbensen SK, Schlax MG, Thum N, Freilich MH, Wentz FJ, Gentemann CL, McPhaden MJ, Schopf PS (2001) Observations of coupling between surface wind stress and sea surface temperature in the eastern tropical Pacific. J Clim 14:1479–1498

Chelton DB, Schlax MG, Samelson RM (2007) Summertime coupling between sea surface temperature and wind stress in the California current system. J Phys Oceanogr 37:495–517

Efron B, Tibshirani R (1994) An introduction to the bootstrap. Chapman and Hall, New York

Faber NM (2002) Uncertainty estimation for multivariate regression coefficients, Chemometr. Intell Lab Syst 64(2002):169–179

Falvey M, Garreaud R (2009) Regional cooling in a warming world: recent temperature trends in the SE Pacific and along the west coast of subtropical South America (1979–2006). J Geophys Res 114:D04102. doi:10.1029/2008JD010519

Garreaud R, Falvey M (2009) The coastal winds off western subtropical South America in future climate scenarios. Int J Climatol 29:543–554

Garreaud R, Munoz R (2005) The low-level jet off the subtropical west coast of South America: structure and variability. Mon Wea Rev 133:2246–2261

Gastineau G, Soden BJ (2009) Model projected changes of extreme wind events in response to global warming. Geophys Res Lett 36:L10810. doi:10.1029/2009GL037500

Gastineau G, Le Treut H, Li L (2008) Hadley circulation changes under global warming conditions indicated by coupled climate models. Tellus A 60:863–884

Halpern D (2002) Offshore Ekman transport and Ekman pumping off Peru during the 1997–1998 El Nino. Geophys Res Lett 29(5):1075. doi:10.1029/2001GL014097

Held IM, Soden BJ (2006) Robust responses of the hydrological cycle to global warming. J Clim 19:5686–5699

Jin X, Dong C, Kurian J, McWilliams JC, Chelton DB, Li Z (2009) SST-wind interaction in coastal upwelling: oceanic simulation with empirical coupling. J Phys Oceanogr 39(11):2957

Kalnay E, Kanamitsu M, Kistler R et al (1996) The NCEP/NCAR 40-year reanalysis project. Bull Amer Meteor Soc 77:437–471

Marti O, Braconnot P, Dufrense JL et al (2010) Key features of the IPSL ocean atmosphere model and its sensitivity to atmospheric resolution. Clim Dyn 34:1–26

Minvielle M, Cassou C, Terray L, Bourdalle-Badie R (2010) A statistical-dynamical scheme for ocean downscaling in the Atlantic. Part II: methodology, validation and application to high resolution ocean models. Clim Dyn. doi:10.1007/s00382-010-781-7

Najac J, Boé J, Terray L (2009) A multi-model ensemble approach for assessment of climate change impact on surface winds in France. Clim Dyn 32:615–634

Pryor SC, Schoof JT, Barthelmie RJ (2005) Empirical downscaling of wind speed probability distributions. J Geophys Res 110:D19109. doi:10.1029/2005JD005899

Pryor SC, Schoof JT, Barthelmie RJ (2006) Winds of change? Projections of near-surface winds under climate change scenarios. Geophys Res Lett 33:L11702. doi:10.1029/2006GL026000

Renault L (2008) Impact of atmospheric coastal jets on upwelling in the Humboldt Current System. PhD thesis, Toulouse III University (in French)

Renault L, Dewitte B, Falvey M, Garreaud R, Echevin V, Bonjean F (2009) Impact of atmospheric coastal jets on SST off central Chile from satellite observations (2000–2007). J Geophys Res 114:C08006. doi:10.1029/2008JC005083

Sailor DJ, Hu T, Li X, Rosen J (2000) A neural network approach to local downscaling of GCM output for assessing wind power implications of climate change. Renew Energy 19:359–378

Salameh T, Drobinski P, Vrac M, Naveau P (2009) Statistical downscaling of near surface wind field over complex terrain in southern France. Meteorol Atmospheric Phys 103(1–4):253–265

Seo H, Miller AJ, Roads JO (2007) The Scripps coupled ocean–atmosphere regional (SCOAR) model, with applications in the eastern pacific sector. J Clim 20:381–402

Small J, deSzoeke SP, Xie SP, O'Neill L, Seo H, Song Q, Cornillon P, Spall M, Minobe S (2008) Air–sea interaction over ocean fronts and eddies. Dyn atmospheres Oceans 45:274–319

Solomon S, Qin D, Manning M, Chen Z, Marquis M, Averyt KB, Tignor M, Miller HL (eds) (2007) Climate change 2007: the physical science basis. Cambridge University Press, 996 pp

Uppala S, KÅllberg PW, Simmons AJ et al (2005) The ERA-40 reanalysis. Quart J Roy Meteor Soc 131:2961–3012

Vecchi GA, Soden BJ (2007) Global warming and the weakening of the tropical circulation. J Clim 20(17):4316–4340

von Storch H (1999) On the use of "inflation" in downscaling. J Clim 12:3505–3506

von Storch H, Zwiers FW (2004) Statistical analysis in climate research. Cambridge University Press, New York

Worley SJ, Woodruff SD, Reynolds RW, Lubker SJ, Lott N (2005) Icoads release 21 data and products. Int J Climatol 25(7):823–842. doi:10.1002/joc.1166

Wyrtki K (1975) El Niño–the dynamic response of the equatorial Pacific Ocean to atmospheric forcing. J Phys Oceanogr 5(4):572–584

Xue H, Wang Y, Xie SP (2004) Effects of the andes on eastern pacific climate: a regional atmospheric model study. J Clim 17:587–602

Yeh S-W, Kug S-J, Dewitte B, Kwon M-H, Kirtman BP, Jin F-F (2009) El Niño in a changing climate. Nature 461:511–514